Experimental Demonstration of Cascadable PPLN-Based Inter-Band Wavelength Converters for Band-Switchable Multi-Band Optical Cross-Connect

Haruka Minami [1], Kenta Hirose [1], Takafumi Fukatani [1], Masahiro Nakagawa [1], Takeshi Seki [1], Shimpei Shimizu [2], Takayuki Kobayashi [2], Takushi Kazama [2, 3], Koji Enbutsu [3], Kei Watanabe [2, 3], Takeshi Umeki [2, 3], Takashi Miyamura [1], Takeshi Kuwahara [1]

1 NTT Network Service Systems Laboratories, NTT Corp. 3-9-11 Midori-cho, Musashino-shi, Tokyo, 180-8585, Japan
2 NTT Network Innovation Laboratories, NTT Corp. 1-1 Hikarinooka, Yokosuka, Kanagawa, 239-0547 Japan
3 NTT Device Technology Laboratories, NTT Corp. 3-1 Morinosato Wakamiya, Atsugi, Kanagawa 243-0198 Japan
haruka.minami.wn@hco.ntt.co.jp

Abstract: We experimentally demonstrate the cascadability of PPLN-based inter-band wavelength converters to realize band-switchable multi-band optical cross-connect. Experimental results show that input power optimization can reduce the degradation in transmission quality even when traversing >20 converters.

1. Introduction

Multi-band (MB) optical networking has attracted much attention as a viable solution to cost-effective expand networking capacity. Compared with a conventional multi-band optical cross-connect (MB-OXC) architecture as shown in Fig. 1 (a), that shown in Fig. 1 (b) can select not only the output port but also output wavelength-band by adding all-optical inter-band wavelength converters (AO-WCs) [1, 2]. Specifically, such an AO-WC is assumed to be able to simultaneously convert multiple wavelengths in the transmission band to the other band. The MB transmission with the wavelength-band adaptation enables a significant increase in the traffic volume that can be accommodated [1]. So far, we proposed the MB-OXC with AO-WCs using highly nonlinear fibers and showed a feasibility of the C+L-band OXC supporting 112-Gbit/s DP-QPSK signal transmission [2].

A concern with using AO-WC to implement the wavelength-band adaptation in MB-OXC is transmission quality degradation due to excessive amplified spontaneous emission (ASE) noise and nonlinear distortion induced by wavelength-band conversion on the basis of nonlinear optical effects. Since optical signals are transmitted through multiple optical nodes, it is important to evaluate the cumulative characteristics of such signal degradation due to wavelength-band conversion. The AO-WC using periodically poled lithium niobate (PPLN) waveguides produces little unwanted nonlinear optical effects among wavelength-division multiplexing (WDM) channels and have high-pump-power efficiency, and thus, is good in terms of simultaneously converting a wide-band WDM signal with a high efficiency [3, 4]. Therefore, the PPLN-based AO-WC is expected to provide wavelength conversion with less excessive optical signal-to-noise ratio (OSNR) degradation and nonlinear distortion. Recently, configurations that apply PPLN-based AO-WCs to multi-band Tx/Rx have been proposed and the S-band transmission using only commercial C-band transponders was demonstrated [5, 6].

In this paper, we propose the application of the PPLN-based AO-WCs to the MB-OXC and verify the feasibility of multiple wavelength conversions by a recirculating loop with a pair of the PPLN-based AO-WCs. We experimentally demonstrate that the transmission quality can be maximized by optimizing the input power to the PPLN-based AO-WCs even when traversing more than 20 AO-WCs, which corresponds to the case of traversing more than 10 MB-OXC nodes. This successfully confirms the physical-layer feasibility of implementing the MB-OXC using PPLN-based AO-WCs, enabling wavelength-band adaptation.

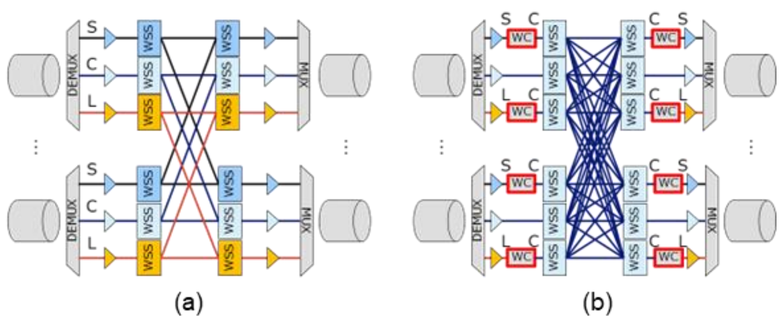

Fig. 1 Architecture of (a) conventional MB-OXC and (b) band-switchable MB-OXC.

2. Experiments

We propose to apply a PPLN-based AO-WC in a band-switching MB-OXC shown in Fig. 1 (b). Figure 2 (a) shows the configuration of C-to-L/L-to-C PPLN-based AO-WC. This was a polarization diversity configuration sandwiched between two polarization beam splitters (PBSs). The PPLN waveguides for second harmonic generation (SHG) converted the pump light of frequency f_p (=190.6 THz) to $2f_p$. The PPLN waveguides for differential frequency generation (DFG) generated an idler of frequency $f_i = 2f_p - f_s$ for each polarization component of an input signal of frequency f_s. The pump light power to the PPLN waveguides for DFG was adjusted so that the conversion efficiency (CE) was ~10 dB. As shown in Fig. 2 (b), the PPLN-based AO-WC can convert the entire C-band (1528.77-1566.62 nm, 50-GHz-spaced 96 ch.) to L-band, and that is the same for L-to-C conversion. To evaluate ASE noise generated with its wavelength conversion process, we measured CE and noise figure (NF) of the PPLN-based WC by comparing the input and output spectra of the PPLN-based WC when −14-dBm CW light was input. Figure 2 (c) shows the measurement results. The average/maximum/minimum values of the CE for C-to-L were 9.9 dB/10.7 dB/8.4 dB, the CEs for L-to-C were 10.4 dB/11.0 dB/9.5 dB, the NFs for C-to-L were 5.0 dB/5.4 dB/4.7 dB, and the NFs for L-to-C were 4.8 dB/5.0 dB/4.6 dB.

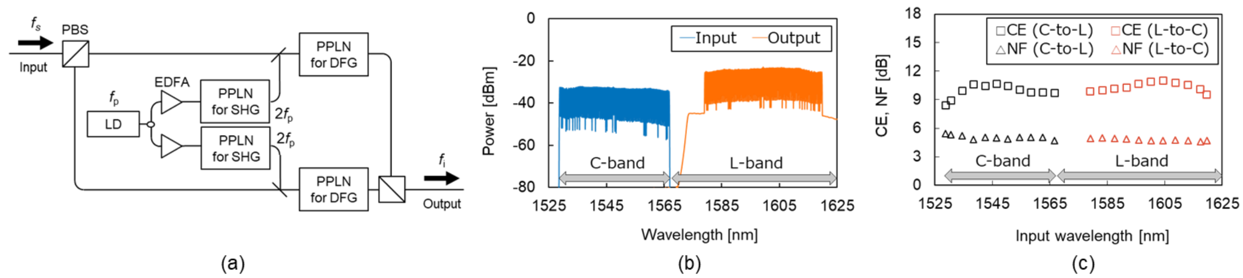

Fig. 2 (a) Configuration, (b) input and output spectrum, and (c) CE and NF characteristics of PPLN-based AO-WC.

In addition to ASE noise, PPLN-based AO-WCs have reported to have nonlinear distortion on the signals due to gain saturation [3, 5] at the high input power region. The crosstalk among WDM channels also occurs due to unwanted wavelength conversion due to high channel power [7]. These distortions induced by the nonlinear optical effects and the ASE noise accumulate with each pass through the PPLN-based AO-WC incorporated in the MB-OXC. To evaluate the accumulative characteristics, we performed the experiments using a recirculating loop. In addition, the dependence of this accumulation characteristic on the input power to the AO-WCs is also evaluated. Figure 3 (a) shows the experimental setup. The measurement channel was 1547.32 nm, which is in the center of the C-band. A 32-Gbaud DP-16QAM was generated using an IQ-modulator (IQM) and a polarization-division multiplexing emulator (PDME). A 50-GHz-spaced 96-ch WDM signal over the entire C-band (1528.77-1566.62 nm) was generated by shaping the ASE light output from an erbium-doped fiber amplifier (EDFA) by using an optical equalizer (OEQ). The recirculating loop consisted of a 40-km G.652.D single mode fiber (SMF), a C-to-L PPLN-based AO-WC 1, an L-to-C PPLN-based AO-WC 2, an OEQ, a loop-synchronous polarization scrambler (LSPS), an optical switch (SW), and three C-band EDFAs. The EDFAs compensated for the losses of optical components in the recirculating loop. The average fiber-input power was –11 dBm/ch, which is sufficiently low power that does not cause fiber nonlinearity such as self-phase modulation. We varied the input power to the PPLN-based AO-WCs using variable optical attenuators (VOAs) placed at the input of the AO-WCs. The input power to the EDFA was set to 0 dBm, independent of the input power to the AO-WCs. In the receiver side, the measurement signal was extracted by using a band-pass filter (BPF) and detected by a polarization-diverse coherent receiver. SNR of the signal was calculated from recovered symbols by offline digital signal processing.

Figure 3 (b) shows dependence of SNR on the input power to the PPLN-based AO-WCs in the cases that the traversed numbers of the AO-WCs were 2, 10, and 20. The optimal input power was 10 dBm (–9.8 dBm/ch) for all the traversed number conditions. The dotted lines in Fig. 3 (b) show the calculated SNRs taking into account only consideration the accumulation of ASE noise with the recirculating, which means that these values correspond to when no nonlinear penalty occurs. These were estimated by premeasured OSNR vs SNR characteristics of back-to-back shown in the inserted figure in Fig. 3 (a) and the received OSNR calculated from the NF of EDFAs and the PPLN-based AO-WCs (see Fig. 2 (c)). The calculated SNR considering only ASE noise improved as the input power increased because of the reduction in received OSNR degradation due to the ASE noise from the PPLN-based AO-WCs. However, the difference between the calculated and measured SNR increased as the input power increased, which would be caused by the nonlinear distortion due to gain saturation and inter-channel crosstalk. This result shows the optimal input power to the PPLN-based AO-WC is determined by both the received OSNR improvement and the nonlinear penalty increase as the input power increased. Figure 3 (c) shows dependence of the measured and calculated SNR on the number of passing the PPLN-based WCs for the input power conditions to the PPLN-based AO-WCs of 0 dBm (–19.8 dBm/ch) and 10 dBm (–9.8 dBm/ch). When the input power was 10 dBm, the nonlinear penalty corresponding to the difference between the calculated and measured SNR increased as the traversed number increased. However, the measured SNRs with the input power of 10 dBm were better than those with the input power of 0 dBm, which had almost no nonlinear penalty, for all the traversed number conditions. These results verified that the optimal input power to the PPLN-based AO-WCs was independent of the traversed number of the AO-WC within 24 traverses. It is suggested that suppression of signal degradation by the input power optimization could help achieve band-switchable MB-OXC.

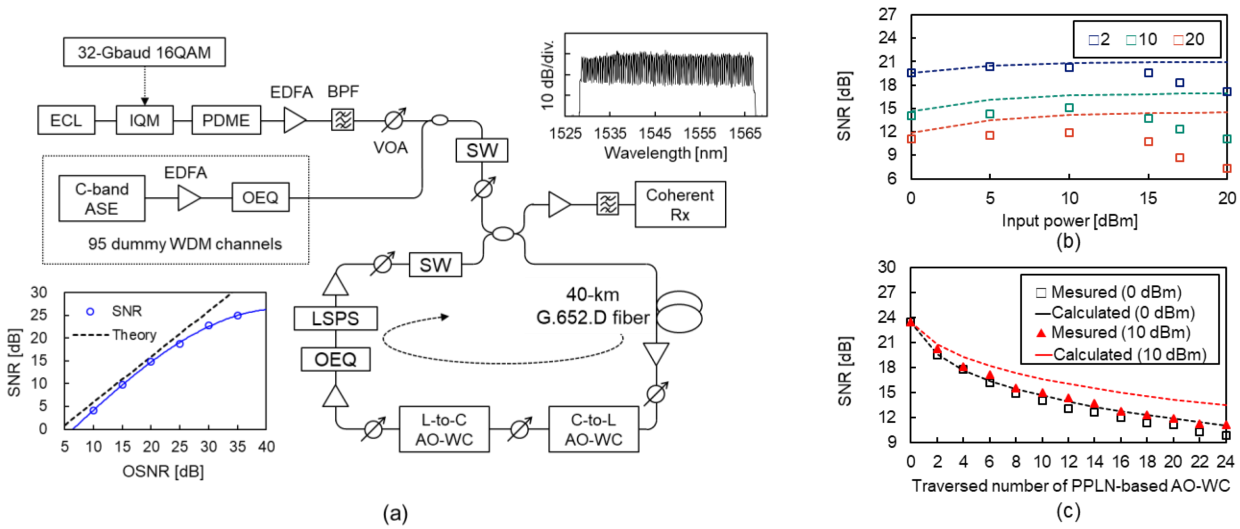

Fig. 3 (a) Experimental setup. Link configuration, OSNR vs SNR characteristic of Tx/Rx, and spectrum of 96-ch WDM signal at 10th lap. (b) Dependence of measured and calculated SNR on the input power to PPLN-based AO-WCs. (c) Dependence of measured and calculated SNR on traversed number of PPLN-based AO-WC.

3. Conclusion

We proposed the MB-OXC configuration using PPLN-based AO-WCs with low excessive signal degradation and experimentally evaluated the cumulative characteristics of signal degradation caused by passing through it. It was shown that transmission quality after passing through the MB-OXC nodes can be maximized by optimizing the input power to the AO-WCs. We also demonstrated that the optimal input power to the PPLN-based AO-WCs was independent of the number of traverses of the AO-WC within 24 traverses, which corresponds to the case of more than 10 traverses of MB-OXC nodes.

References

[1] M. Nakagawa, et al., “Adaptive Link-by-Link Band Allocation: A Novel Adaptation Scheme in Multi-Band Optical Networks,” in Proc. ONDM2021.

[2] H. Kawahara, et al., “Experimental Demonstration of Wavelength-Selective Band/Direction-Switchable Multi-Band OXC Using an Inter-Band All-Optical Wavelength Converter,” ECOC2020, Tu1H-5.

[3] T. Kobayashi, et al., “Wide-band inline-amplified WDM transmission using PPLN-based optical parametric amplifier,” J. Lightwave Technol., **39**, pp. 787–794 (2021).

[4] S. Shimizu, et al., “PPLN-based optical parametric amplification for wideband WDM transmission,” J. Lightwave Technol., **40**, pp. 3374-3384 (2022).

[5] T. Kato, et al., “WDM Transmission in S-Band Using PPLN-Based Wavelength Converters and 400-Gb/s C-Band Real-Time Transceivers,” OECC/PSC 2022, WA3-4.

[6] T. Kato, et al., “S+C+L-Band WDM Transmission Using 400-Gb/s Real-Time Transceivers Extended by PPLN-Based Wavelength Converter,” ECOC2022, We4D.4.

[7] T. Kazama, et al., “Low-Parametric-Crosstalk Phase-Sensitive Amplifier for Guard-Band-Less DWDM Signal Using PPLN Waveguides,” J. Lightwave Technol., **35**, pp. 755-761 (2017).